Article

Previous Article | Next Article | Table of Contents

Development of Arrayed Colonic Organoids for Screening of Secretagogues Associated with Enterotoxins

Dulan B. Gunasekara†∥, Matthew DiSalvo‡∥, Yuli Wang†, Daniel L. Nguyen†, Mark I. Reed†, Jennifer Speer†, Christopher E. Sims†, Scott T. Magness‡§, and Nancy L. Allbritton*†‡

†Department of Chemistry and §Division of Gastroenterology and Hepatology, Department of Medicine, University of North Carolina at Chapel Hill, Chapel Hill, North Carolina 27599, United States

‡ Joint Department of Biomedical Engineering, University of North Carolina at Chapel Hill and North Carolina State University, Chapel Hill/Raleigh, North Carolina 27599/27607, United States

Anal. Chem., **2018**, *90* (3), pp 1941–1950

DOI: 10.1021/acs.analchem.7b04032

Publication Date (Web): December 27, 2017

*E-mail nlallbri@unc.edu; tel +1-919-966-2291; fax +1-919-962-2388.

Abstract

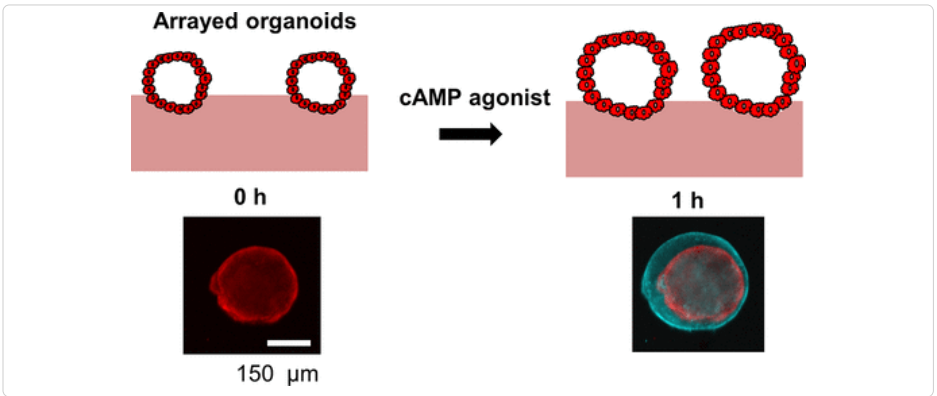

Enterotoxins increase intestinal fluid secretion through modulation of ion channels as well as activation of the enteric nervous and immune systems. Colonic organoids, also known as colonoids, are functionally and phenotypically similar to in vivo colonic epithelium and have been used to study intestinal ion transport and subsequent water flux in physiology and disease models. In conventional cultures, organoids exist as spheroids embedded within a hydrogel patty of extracellular matrix, and they form at multiple depths, impairing efficient imaging necessary to capture data from statistically relevant sample sizes. To overcome these limitations, an analytical platform with colonic organoids localized to the planar surface of a hydrogel layer was developed. The arrays of densely packed colonoids (140 μm average diameter, 4 colonoids/mm^2) were generated in a 96-well plate, enabling assay of the response of hundreds of organoids so that

analysis platform efficiently tracked over time swelling due to forskolin and fluid movement across the cell monolayer stimulated by cholera toxin. The platform was used to screen compounds associated with the enteric nervous and immune systems for their effect on fluid movement across epithelial cells. Prostaglandin E2 promoted increased water flux in a subset of organoids that resulted in organoid swelling, confirming a role for this inflammatory mediator in diarrheal conditions but also illustrating organoid differences in response to an identical stimulus. By allowing sampling of a large number of organoids, the arrayed organoid platform permits identification of organoid subpopulations intermixed within a larger group of nonresponding organoids. This technique will enable automated, large-scale screening of the impact of drugs, toxins, and other compounds on colonic physiology.

Infectious diarrheas caused by bacterial production of enterotoxins are common diseases worldwide. Enterotoxins such as cholera toxin, produced by the bacterium *Vibrio cholerae*, interact with intestinal epithelial cells to increase the movement of water and ions into the intestinal lumen, the consequence of which is severe diarrhea.(1) Cholera toxin acts through a series of steps that include binding of the toxin to the surface of epithelial cells, endocytosis, and a series of enzymatic reactions that result in release of cholera toxin A1 (CTA1) chain, which binds to the intracellular protein ADP-ribosylation factor 6 (Arf6), resulting in CTA1 activation.(2) Through an additional series of enzymatic steps, CTA1 increases the activity of the Gs α subunit (Gαs) proteins, leading to increased adenylyl cyclase activity that results in an elevation in 3′,5′-cyclic adenosine monophosphate (cAMP) concentration more than 100-fold higher than normal, leading to increased activity of protein kinase A (PKA). Phosphorylation of the cystic fibrosis transmembrane conductance regulator (CFTR) chloride channel proteins by PKA then leads to ATP-mediated efflux of chloride ions, resulting in the movement of H_2O as well as sodium, potassium, and bicarbonate ions into the intestinal lumen.(1, 3, 4) The calcium-activated chloride channel (CLCA) can also cause fluid migration in response to toxin-mediated increase in the concentration of intracellular Ca^{2+}.(5) Other enterotoxins also secreted by the *Vibrio* bacterium are known to activate the enteric nervous and immune systems, producing agonists such as prostaglandins, acetylcholine, and histamine, which can also participate in intestinal ion and water movement through intracellular cAMP or Ca^{2+} signaling.(1) The synergistic impact of enterotoxin-mediated effects increases intestinal secretion, yielding rapid and cumulative fluid loss of up to 2 L/h into the intestine, causing severe dehydration that may result in death.(6)

To study intestinal ion secretion and fluid movement, tissue-cultured tumor cell lines are often used as surrogate intestinal cells. However, the genetic profile and functional properties of tumor cells do not match those of primary tissue.(7) Intestinal organoids derived from primary cells offer a more accurate functional model of in vivo tissue physiology compared to tumor cells.(8, 9) Proliferative organoids are readily cultured from crypts or stem cells isolated from the intestine and are maintained by culture within a thick layer of hydrogel (typically Matrigel) in the presence of a medium rich in growth factors.(10) The organoids possess all cell types of the intestine, including stem/proliferative cells, enterocytes, and goblet cells. These cells form a monolayer surrounding a central lumen and are polarized so that their luminal surface faces into the central cavity while the basal cell surface makes contacts with the extracellular matrix proteins within the surrounding hydrogel. This cell polarity enables the organoids to retain many physiologic functions such as transport of ions across the monolayer.(8, 11) Contact between the basal, cell-surface proteins and the extracellular matrix is thought to be required to provide the correct mechanical and chemical environment for proper organoid formation, monolayer polarity, and ion transport function.(8, 12, 13)

Intestinal organoids have been used for nutrient,(14) P-glycoprotein (P-gp),(15) and ion transport assays.(11) When ions are secreted by the monolayer, water follows by a passive mechanism termed osmosis. When sufficient numbers of ions are secreted, the increase in luminal volume due to water movement results in swelling of these spheroidal structures and an increase in the organoid's cross-sectional area. This area increase can be measured directly(11, 16) or indirectly(17) when imaged by microscopy. This phenomenon has enabled intestinal organoids to be used in the study of drug effects, genetic mutation impact, and toxin effect on ion secretion in the organoids.(11, 16, 18-20) However, embedding the organoids fully within a hydrogel poses a number of challenges to increasing the assay throughput.(21) The organoids cultured in a Petri dish or multiwell plate are typically positioned at random locations along the *x*, *y*, and *z* axes of the thick hydrogel layer, leaving the organoids in varying image planes when viewed by microscopy. This creates two challenges that severely limit assay speed: (i) organoids that are out of focus

Published online 27 December 2017
Published in print 6 February 2018

would increase the numbers of organoids per well that are suitable for assay and increase experimental throughput. A second disadvantage is that compounds and drugs must diffuse through the hydrogel to access the organoid. Interactions of molecules with Matrigel can impose a time delay in compounds reaching the organoid or decrease the concentration of compound at the organoid's location. Thus, compound–Matrigel interactions represent an uncontrolled variable in organoid experiments.

We describe the development of a method to create a planar array of colonoids where the colonoids are located on the surface of a hydrogel and compatible with automated image-based assays. Properties of the surface-positioned colonoids were compared to those of hydrogel-embedded organoids. Software to perform organoid segmentation and separation of nearby organoids, as well as identification of the colonoid location, was implemented. An automated analysis pipeline identified and quantified the properties of organoids over time and was compared to manual identification and measurement. Colonoid swelling in response to forskolin, cholera toxin, and physiologic molecules was assessed to characterize the extent and heterogeneity of swelling in a population of organoids as well as the rate of fluid movement across the organoid wall. This approach should enable efficient, large-scale screening of the impact of drugs, toxins, and other compounds on colonoid physiology.

Experimental Section

Materials

Polystyrene 96-well plates were purchased from Denville Scientific, Inc., Holliston, MA. Transwells, Matrigel, ethylenediaminetetraacetic acid (EDTA), 4-(2-hydroxyethyl)-1-piperazineethanesulfonic acid (HEPES), and gentamicin were purchased from Corning. Dimethyl sulfoxide (DMSO) was acquired from Santa Cruz Biotechnology, Dallas, TX. Optimum cutting temperature (OCT) formulation was obtained from Tissue-Tek, Sakura Finetek USA, Inc., Torrance, CA. Na_2HPO_4, KH_2PO_4, NaCl, KCl, advanced Dulbecco's modified Eagle medium (DMEM)/F-12 medium, dithiothreitol (DTT), GlutaMAX, penicillin, and streptomycin were from Thermo Fisher Scientific, Waltham, MA. Epidermal growth factor (EGF), *N*-acetylcysteine, sucrose, D-sorbitol, cholera toxin and its subunit B, bradykinin, prostaglandin E2, adenosine, serotonin, acetylcholine, and histamine were purchased from Sigma, St. Louis, MO. Vasoactive intestinal peptide was purchased from AnaSpec, Fremont, CA. Fetal bovine serum (FBS) was obtained from Atlanta Biologicals, Flowery Branch, GA. Collagenase type IV was purchased from Worthington Biochemical Corp., Lakewood, NJ. Information for staining and assay kits is provided in the relevant subsections.

Isolation of Crypts from Mouse Colon and Initial Culture

The cytomegalovirus enhancer plus chicken actin promoter (CAG)-DsRed mouse model, in which all cells expressed the DsRed fluorescent protein, and wild-type (WT) mice were used for experiments.(22, 23) All experiments and animal usage were in compliance with the University of North Carolina animal care protocol and were approved by the Institutional Animal Care and Use Committee (IACUC). Mice heterozygous for DsRed expression were bred on a CD-1 background, and WT mice were bred on a C57BL/6 background. Mice (male and female, ages 6–10 weeks) were humanely euthanized by a lethal dose of isoflurane followed by cervical dislocation under the UNC IACUC-approved protocol 13-200. A detailed procedure for crypt isolation and culture was previously reported.(24, 25) Briefly, a colon was surgically extracted from a mouse following euthanasia. The colon was then opened longitudinally and incubated with EDTA (2 mM) and DTT (0.5 mM) in isolation buffer (5.6 mM Na_2HPO_4, 8.0 mM KH_2PO_4, 96.2 mM NaCl, 1.6 mM KCl, 43.4 mM sucrose, and 54.9 mM D-sorbitol at pH 7.4) for 75 min at room temperature prior to isolation of crypts. Then the tissue was vigorously shaken in a conical tube with isolation buffer to release the crypts from the underlying stroma. Released crypts were pelleted by centrifugation and mixed with Matrigel (2500 crypts in 100 μL of Matrigel) on ice (4 °C). Aliquots (10 μL) of this mix were plated in wells of a 24-well plate, and the plate was immediately inverted to prevent any contact between tissue pieces and the polystyrene surface. The Matrigel was then cured at 37 °C in a cell culture incubator for 15 min. These cultures were subcultured up to 5 times.

Both embedded and arrayed cultures were grown in medium rich in growth factors, termed stem cell medium (SM). SM was prepared by diluting Wnt 3A, R-spondin 2, and Noggin conditioned medium in advanced DMEM/F-12 basal medium and adding necessary nutrients and buffers. Final concentrations of each growth factor were Wnt 3A (80 ng/mL), R-spondin 2 (38 ng/mL), Noggin (36 ng/mL), GlutaMAX (1x), HEPES (10 mM), *N*-acetylcysteine (1.25 mM), murine EGF (50

concentration of Wnt 3A was determined by a Wnt 3A enzyme-linked immunosorbent assay (ELISA) kit (LifeSpan BioSciences, Inc., Seattle, WA). R-spondin 2 and Noggin growth factor concentrations were measured as described previously.(22) The assay medium contained the same nutrients and buffers in similar concentrations to SM except Wnt 3A (26 ng/mL), R-spondin 2 (30 ng/mL), and Noggin (56 ng/mL).

Generation of Arrayed Colonoids

A planar biomimetic scaffold composed of Matrigel (protein concentration 9.2 mg/mL) was prepared in a multiwell plate. For a 96-well plate, 75 μL of Matrigel was dispensed to each well, and for 12-well Transwell plates, 200 μL of Matrigel was dispensed to produce a Matrigel layer 2.4 mm thick. The plate was centrifuged for 1.5 min at 2000 relative centrifugal force (rcf) at 1 °C. The plate was transferred to a 37 °C cell culture incubator for 10 min for Matrigel gelation. To grow organoids on these surfaces, colonoids grown in a Matrigel patty were isolated by incubation with collagenase (type IV, 500 units/mL) to break up the Matrigel. After release of colonoids from the hydrogel, the colonoids were gently mechanically dissociated. Fragmented colonoids (≤50 μm in diameter) containing cells derived from a WT or CAG Ds-Red mouse were added to the surface of a Matrigel-filled well as a suspension (120 000 cells) in SM. The number of cells in the isolated colonoids was calculated by CellTiter-Glo luminescence cell viability assay (Promega US, Madison, WI) according to the manufacturer's protocol. Over the first 24 h in culture, colonoid fragments (≤50 μm diameter) were allowed to adhere to the Matrigel layer. Over the course of the subsequent 2–3 days, these fragments developed into colonoids ≥100 μm in diameter. Arrays were imaged on a Nikon Eclipse TE300 inverted epifluorescence microscope with an estimated objective depth of field of >59 μm [numerical aperture (NA) 0.13] for comparison with three-dimensional (3D) embedded cultures. The viability of colonoids after culturing 72 h on an array was measured by use of propidium iodide (PI) as a marker of cells' death and Hoechst 33342 as a counterstain. After 72 h of culture, 100% of the colonoids were viable.

Colonoid Characterization

Colonoids were grown on the surface of Matrigel layered onto the membrane of a 12-well Transwell insert. After the colonoids were cultured for 3 days, the array was fixed with 4% paraformaldehyde for 25 min. The array was incubated with 30% sucrose for 3 h and kept in OCT formulation overnight. The membrane was cut out of the inset, and the tissue was sectioned with a cryostat to obtain 10 μm thick slices. These slices were stained with fluorescently labeled phalloidin for F-actin (ActinGreen 488, Molecular Probes, Thermo Fisher Scientific, Waltham, MA) and Hoechst 33342 and then imaged by fluorescence microscopy.

Cell Lineages in Arrayed Colonoids

To mark S-phase cells, 5-ethynyl-2′-deoxyuridine (EdU, 10 μM in SM) was incubated on the arrays for 4 h. The arrays were then fixed in 4% paraformaldehyde for 20 min and incubated with 0.5% Triton X-100 for 20 min to facilitate diffusion of the labeling reagents into the cells. EdU-marked cells were then stained by use of a Click-iT EdU Alexa Fluor 647 imaging kit (Thermo Fisher Scientific, Waltham, MA). Next, the goblet cells were stained with rabbit anti-mucin2 (α-Muc2, 1:200, Santa Cruz Biotechnology, Inc., Dallas, TX, sc-15334).(26) A secondary antibody, Alexa Fluor 488 α-rabbit (1:500, Jackson Immunoresearch, West Grove, PA, 711-545-152), was used to fluorescently label the primary antibody. Stained colonoids were imaged on a Nikon Eclipse TE300 inverted epifluorescence microscope with an estimated objective depth of field of >11 μm (NA 0.3).

Automated Fluorescence Imaging of Arrayed Colonoids

Automated imaging of arrayed colonoids was performed on an Olympus IX81 inverted epifluorescence microscope with a 4× objective (Olympus UPlanFL N, NA 0.13 with an estimated objective depth of field of 40 μm) and a CoolSNAP HQ2 charge-coupled device (CCD) camera (Photometrics, Tucson, AZ) or Hamamatsu Flash 4.0 VZ (Hamamatsu, Japan). Colonoids in this study were fluorescently labeled, either by labeling with Hoechst 33342 to stain DNA or by using colonoids derived from CAG-DsRed mouse model in which all cells expressed the DsRed fluorescent protein. For fluorescence imaging of DSRed and Hoechst 33342, Chroma ET-YFP 49003 and Chroma ET-DAPI 49000 filters were used, respectively. The microscope was equipped with a humidified incubation chamber to maintain an environment at 5% CO_2 and 37 °C. All automated image acquisition was controlled by a custom MATLAB program (MATLAB 2014b, The MathWorks, Inc., Natick, MA) harnessing Micro-Manager microscopy software. Individual wells within plates were imaged with overlapping fields of view (i.e., 6 × 4 image tiling to cover a single well of a 96-well plate).

Despite the curved shape of the Matrigel substrate (a concave meniscus measuring 595 ± 84 μm

compensate for any curvature of the Matrigel surface upon which the arrayed colonoids were cultured. First, prior to image acquisition, an autofocus scan of the colonoid array was performed to determine focal positions for each desired imaging region throughout the array. A software-based autofocus was used that maximized the standard deviation of the pixel intensity in fluorescence images of the colonoids. To further guarantee well-focused images, 40% image overlap was employed during mosaicking and only the highly focused, central nonoverlapped portion of each image was used for subsequent analysis. Once the imaging positions were determined by utilizing these approaches, a 15 mm^2 area composed of 4 × 6 images with 40% overlap between fields was acquired for each well in 22 s. The 15 mm^2 area was chosen to avoid imaging too close to the well walls (well area 32 mm^2 for 96-well plates).

Image Analysis and Assay Metrics

All image analyses were performed with custom MATLAB scripts. The analyses began by forming full-well images by stitching together the well-focused central portions of the images from a well. Colonoids were identified by segmenting the Hoechst or DsRed fluorescent images by use of Otsu's automatic intensity thresholding.(27) For some colonoids the fluorescence labeling was dim, which interfered with basic intensity-thresholded segmentation. For these colonoids, intensity thresholding did not detect the full colonoid boundary, and thus the segmentation was discontinuous when in reality the colonoids had an intact and continuous border. To compensate, a morphological closing operation using a disk of 19 μm radius (3 pixels) was applied. Objects below 100 μm in effective diameter were removed to eliminate debris, dead cells, and organoid fragments. Segmentation holes were filled and adjacent colonoids were separated by a geometric watershed transform.(28) Colonoid centroids, areas, and mean fluorescence intensities were automatically recorded within the colonoid boundaries identified in the final segmentation masks.

To track colonoid properties over time, an algorithm was constructed to match the colonoids in the images acquired at different time points. Every identified colonoid's centroid was measured at each time point. When colonoids were tracked over time, colonoids whose centroids varied less than 100 μm along the plane of the array and whose areas varied by less than 25% between time points were considered to be the same colonoid. In the event of temporal gaps in the tracking of a colonoid, the algorithm linearly interpolated colonoid measurements for up to two time points. Colonoids with three or more untracked time points were excluded from analysis.

Several metrics were used to quantify changes in colonoid size over time. The magnitude of the change in a colonoid's area was measured as the percent area increase relative to the initial area (ΔA, expressed as a percentage) or maximal value of ΔA during the assay time (ΔA_{max}, expressed as a percentage). The initial rate of size increase of colonoids was quantified as the slope of a linear fit ($R^2 > 0.85$) of area as a function of time. With the assumption that colonoids are spherical and swell isotropically, area rates of change could be converted into net fluid flux occurring between time points 1 and 2 according to

$$\text{flux}_{1,2} = \frac{\left(\frac{V_2}{A_2} - \frac{V_1}{A_1}\right)}{t_2 - t_1}$$

where V_i and A_i represent the colonoid volume and colonoid surface at times 1 and 2 (t_i). To cluster colonoid subpopulations, an expanded 10-dimensional data set was extracted per colonoid (see Supporting Information). Supervised clustering to classify individual colonoids into nonresponsive (i.e., negative control-like) or responsive (i.e., positive control-like) groups was performed with a binary linear support vector machine classifier (MATLAB's fitcsvm).(29) Unsupervised clustering was performed via *k*-means clustering with $k = 2$. For classification, each dimension of the data was centered and scaled by the mean and standard deviation. Classification accuracy was estimated by five cross-validation folds.

cAMP-Stimulated Transport

Colonoids at day 2 of growth on the array were used for all fluid transport assays since these colonoids are composed primarily of stem/proliferative cells, which are thought to play a major role in fluid secretion.(30) Wild-type colonoids were stained with Hoechst 33342 (2 μM in assay medium) for 25 min. Forskolin was used for activation of adenylyl cyclase to increase the intracellular cAMP concentration. Forskolin (1 μM), cholera toxin (CT, 5 or 0.5 μg/mL) or subunit B of CT (C-B, 5 or 0.5 μg/mL) in assay medium was added to arrayed colonoids, which were then immediately imaged every 3 min for 1–1.5 h. DMSO, in an amount equivalent to that in added forskolin, was added to control wells. The viability of colonoids after 48 h on the array with and

forskolin- and DMSO-treated samples.

Investigation of Fluid Movement Using Compounds of the Enteric Nervous and Immune Systems

Eight compounds that are known to be associated with cAMP- or Ca^{2+}-regulated ion transport were assessed for their ability to induce fluid movement into the colonoids, leading to colonoid swelling (Table S1). All compounds except forskolin were dissolved in 1× phosphate-buffered saline (PBS) or distilled water and diluted 1000× in assay medium prior to addition to the colonoids. Forskolin was dissolved in DMSO and diluted 1000× in assay medium. Addition of assay medium or DMSO (0.1%) was used as a control. After being cultured for 2 days in SM, colonoids were stained with Hoechst 33342 for 25 min. The medium in each well was then replaced with the appropriate experimental or control medium and the plate was transferred to the microscope for time-lapse fluorescence imaging every 3.6 min for 32 min. Compound screening was performed in triplicate by culturing arrayed colonoids in three 96-well plates utilizing 16 wells within each plate: one for each of the eight compounds to be screened; one each for the forskolin and cholera toxin positive and negative controls, respectively; five for the assay medium controls; and one for the DMSO control. To control for plate-to-plate variance, each plate used a random well order for the compounds.

Statistical Analysis

Unless otherwise specified, data are presented as the sample mean and standard deviation. Two-tailed *t*-tests were utilized for comparisons between two groups. Statistical analyses of multiple experimental groups and controls were performed by one-way analysis of variance (ANOVA) and Tukey's test for multiple comparisons. For statistical analysis of multiple experimental groups between embedded and arrayed organoids, two-way unbalanced ANOVA with type III sum of squares and Tukey's test for multiple comparisons were used. All statistical tests were performed at a significance level of 0.05 and were computed by MATLAB or GraphPad Prism (GraphPad Software, Inc. La Jolla, CA). G*Power software (Heinrich Heine University) was used for a priori sample size determination based on a two-tailed *t*-test for differences in ΔA_{max} of two groups with $\alpha = 1 - \beta = 0.05$.

Box-and-whisker plots were used to show ΔA_{max} (%) of colonoids. The small box indicates the mean of the data, the bar shows the median, and the upper and lower boxes represent the 75th and 25th percentiles of the data, respectively. The whiskers extend to the fifth and 95th percentiles, and × denotes outliers. For all statistical comparisons, *p*-values were represented as follows: * for $p < 0.05$, ** for $p < 0.01$, *** for $p < 0.001$, and **** for $p < 0.0001$.

Results and Discussion

Generation of a Colonoid Array and Its Characterization

To generate colonoid arrays, a protocol similar to that used to create acinar cultures from tumor cell lines was adapted for primary intestinal epithelial organoids.(13, 31) Colonoid fragments possessing proliferative cells were plated on the surface of a layer of polymerized Matrigel. Cells in the colonoids adhered to the upper surface of the Matrigel and expanded in size while remaining attached to the surface (Figure 1A,B). Under these conditions, 24% ± 11% ($n = 19$) of the colonoid diameter was embedded within the Matrigel, with the remainder extending above the Matrigel surface into the overlying medium (Figure 1D). None of the colonoids ($n = 70$) on the Matrigel surface overlapped in the Z dimension. In contrast, colonoids embedded in conventional 3D cultures were frequently found to overlap one another and reside in multiple focal planes throughout the gel (Figure S1). The polarity of the cell layer surrounding the colonoid lumen was investigated by fixing and cryosectioning the colonoids after 3 days of growth, followed by staining F-actin with fluorescently labeled phalloidin. F-actin was localized to the inner surface of the colonoid lumen, suggesting that the actin-rich microvilli were also located on the luminal organoid surface and that the organoids were properly polarized (Figure 1C).(32)

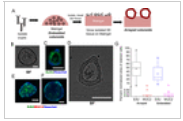

Figure 1. Generation and characterization of arrayed colonoids and comparison to embedded colonoids. (A) Work flow for generating the arrayed colonoids. (B) Bright-field image of an individual colonoid within the array. (C) F-actin (green) and Hoechst (blue) stained cryosectioned image of an arrayed colonoid. (D) Cryosectioned bright-field image of an arrayed colonoid. (E, F) EdU (green), MUC2 (red), and Hoechst (blue) stained images of (E) arrayed and (F) embedded colonoids. (G) Percent normalized area positive for EdU or MUC2 fluorescence in arrayed and embedded organoids. All scale bars represent 75 μm.

vivo. To identify cell lineages present in the arrayed colonoids, arrayed and embedded colonoids were pulsed with EdU to identify S-phase cells and immunostained for mucin 2 (MUC2) to identify the differentiated goblet cells. Colonoids were imaged with a fluorescence microscope. The area of the colonoid displaying EdU-based or MUC2 immunofluorescence was quantified and normalized to the total area of the organoid, that is, the organoid image area positive for Hoechst 33342 fluorescence. Colonoids that were cultured on the arrays in a medium rich in growth factors (SM) displayed an EdU+/Hoechst area of 47.2% ± 24.5% (n = 27), suggesting large numbers of S-phase or proliferative cells (Figure 1E,G). The MUC2+/Hoechst area was 0.5% ± 1.1% (n = 29), indicating that few of the differentiated goblet cells were present under these culture conditions (Figure 1E,G). For comparison, Matrigel-embedded colonoids cultured in the presence of the SM possessed an EdU+/Hoechst area of 34.6% ± 22.0% (n = 25) that was not significantly different from that of the arrayed colonoids (p = 0.852) (Figure 1F,G). Similarly, the MUC2+/Hoechst area for the embedded colonoids (0.3% ± 0.9%, n = 25) was not significantly different than that of the arrayed colonoids (p = 0.486) (Figure 1F,G). Thus, the arrayed colonoids displayed similar numbers of proliferative and differentiated cells to those found in the embedded colonoids, suggesting that the two organoid culture systems were similar. Additionally, the large standard deviation in the area of EdU uptake and MUC2 immunostaining suggested that the colonoids might be quite heterogeneous in their properties in both culture systems.

Automated Assay of Colonoid Arrays

Since the colonic organoids displayed heterogeneous behavior, significant sample sizes would likely be required to identify subpopulations and/or responses to some compounds. Thus, automated microscopy and image analysis were implemented so that hundreds of colonoids could be assayed per experiment. A motorized microscope acquired a grid of images spanning each well of a 96-well plate (Figure 2A). As the colonoids lay above the hydrogel surface and the structures did not overlap, autofocus routines could be applied to rapidly image the colonoid arrays (22 s/well). The images of each well were stitched together, followed by application of an automated analysis pipeline (Figure 2A,B). The colonoids were segmented by use of Otsu's method for thresholding to create a mask for subsequent fluorescence measurements.(27) The masks were size-filtered to remove objects less than 60 μm in diameter, and adjacent colonoids were separated by a watershed transform.(28) Colonoid centroids, areas, and mean fluorescence intensities were then quantified for the masked regions, and these features as well as the colonoid location were tracked over time.

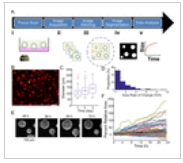

Figure 2. Automated imaging and image analysis. (A) Work flow of automated image acquisition and analysis. (i) Arrayed colonoids are imaged over time on a motorized wide-field microscope. (ii) A top-view image of each colonoid is obtained. (iii) Images of the colonoids are stitched into a single image per well (black dashed–dotted line represents well perimeter). (iv) Colonoids are segmented by automated image analysis to produce a binary map of each colonoid. (v) Assay metrics such as colonoid size over time are extracted. (B) Stitched, full-well image showing DsRed fluorescence of colonoids after 3 days of growth on the array. Scale bar represents 500 μm. (C) Box-and-whisker distributions of colonoid diameter over time. (D) Histogram of percent of colonoids versus their percent area rate of change (%/h). (E) Time series of DsRed fluorescence images of the single colonoid indicated by the yellow arrow in panel B. (F) Change in colonoid cross-sectional area over time, relative to time zero. Each trace represents a single colonoid (n = 62 colonoids), with the population median colonoid swelling represented by the black trace.

To develop the automated platform, murine colonoids expressing DsRed were cultured on the arrays and imaged over 3 days. The wells contained a total of 214 colonoids (n = 3 wells). The median colonoid diameter increased from 105.0 ± 12.8 to 139.0 ± 6.7 μm (p < 0.02) over the 3-day culture time (Figure 2C–E). Between days 2 and 3, the majority of the colonoids (52.6% ± 6.5%) experienced ≤25% increase in image plane area (Figure 2D, Video S1). The colonoids were nearly stationary over this time with an average linear velocity of 2.8 ± 0.3 μm/h. A small percentage (9.4%) of the colonoid population displayed >75% increase in image area during the 24 h time, with the fastest growing colonoid expanding in area from 17 850 to 36 237 μm^2 (equivalent diameter increase from 151 to 215 μm). Most of the colonoids (95%) displayed area growth rates <4.3%/h and absolute area growth rates <479 μm^2/h.

The performance of automated image analysis of colonoid area and position was evaluated from image data acquired between days 2 and 3 of culture (Figure 2F). The automated image analysis routines segmented and tracked 72.6% ± 7.9% of the wells' colonoids (154 colonoids across 3 wells). A goal of this work was to segment the entire colonoid without including adjacent colonoids

expense of excluding 22.3% ± 7.7% (49 colonoids in total) of the colonoids based upon thresholds of allowable colonoid diameter, swelling rates, and centroid velocities. Both inaccurate measurements and colonoid exclusion occurred predominantly when the colonoids were clustered too densely for successful segmentation or possessed regions that fell below the fluorescence threshold for the mask. Notably, the array with the lowest colonoid density (4 colonoids/mm^2) exhibited the fewest instances of clustered colonoids and the highest rate of accurate analysis (81.7%). Thus, increasing the density beyond 4–6 colonoids/mm^2 may have diminishing returns on throughput when strict colonoid exclusion criteria are used in image analysis algorithms.

cAMP-Regulated Transport

Intracellular cAMP production initiates ion transport into the intestinal lumen, which is followed by the passive movement of water into the lumen. In the colonoids, ions and fluid move into the enclosed lumen, causing the structure to swell. To assess the cAMP-regulated transport, arrayed colonoids were stained with Hoechst 33342 and stimulated with forskolin (0 or 1 μM), which is commonly used to stimulate the production of cAMP by adenylyl cyclase in cells. The colonoids were imaged over time with the automated platform, and Hoechst fluorescence was used to identify and segment the colonoids. Addition of forskolin to cells resulted in a visible increase in colonoid diameter in less than 1 h, while the DMSO control had no impact on the structures (Figure 3A,B). Colonoid area was tracked over time to determine net rate of fluid movement across the monolayer of colonic epithelial cells (Figure 3C–E). The percent maximal area increase, ΔA_{max}, of forskolin-treated colonoids was 21.2% [5.3%, 41.9%] (presented throughout as median [25th, 75th percentile]; here n = 66 colonoids) relative to their area prior to forskolin addition (Video S2). In contrast colonoids receiving medium or DMSO demonstrated ΔA_{max} values of 1.1% [0%, 2.5%] and 1.4% [0%, 4.1%] (n_{medium} = 63 and n_{DMSO} = 71 colonoids), respectively, which were both statistically different than the response of the forskolin-treated organoids (p < 0.0001 for all comparisons) (Video S3). On average, colonoids achieved 75% of their maximal swelling within 23 min of forskolin addition and 100% of their maximal size within 46 min. The estimated maximal rate of fluid movement in forskolin-treated colonoids during the 1 h assay window was 4.23 ± 3.34 μL·h^{-1}·cm^{-2}, which was significantly different than that estimated for control colonoids (for medium addition, 1.50 ± 2.02 μL·h^{-1}·cm^{-2}; for DMSO addition, 1.75 ± 1.93 μL·h^{-1}·cm^{-2}; p < 0.0001 for all comparisons). The average initial net fluid flux was between 9% and 30% that of the average maximal net fluid flux for colonoids in medium, DMSO, and forskolin. Overall, the fluid transport rate of arrayed colonoids treated with forskolin was comparable to that of 3D embedded cultures under the same conditions, which was 2.16 ± 0.55 μL·h^{-1}·cm^{-2}. These results suggested that cAMP-regulated ion transport followed by passive water movement occurs in the arrayed colonoids.

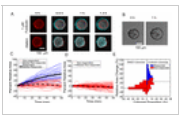

Figure 3. Colonoid swelling initiated by forskolin. (A) Time series of composite DsRed fluorescence images over 1.3 h (time 0, red; other time points, cyan) of a colonoid on an array after addition of forskolin or DMSO at time zero. (B) Bright-field images of a colonoid after addition of forskolin (1 μM) at time zero. (C, D) ΔA of colonoids over time when (C) forskolin (1 μM) or (D) DMSO (0.1%) was added at time zero. k-means clustering with k = 2 was performed to classify the population into nonresponders (red) and responders (blue). (E) Comparison of ΔA versus number of colonoids treated with forskolin or DMSO for the data in panels C and D.

The information-rich images of arrayed colonoids can be used for identification of heterogeneous behaviors after a perturbation, such as application of a drug. For the forskolin-treatment experiment described above, each colonoid's size, swelling magnitude, and swelling kinetics were quantified by a panel of 10 metrics (Supporting Information). To identify treatment-dependent subpopulations of colonoids, the experimental data set, consisting of 66 forskolin-treated, 71 DMSO-treated, and 63 untreated colonoids, was clustered into two groups by k-means clustering (Figure 3C,D). Forskolin-treated colonoids disproportionally fell into the responder cluster, which was composed exclusively of 30 forskolin-treated colonoids. The remaining 36 forskolin-treated and 134 non-forskolin-treated organoids clustered into a nonresponder group. Forskolin-treated responders and nonresponders possessed ΔA_{max} values of 47.7% [35.8%, 63.7%] and 7.6% [4.0%, 20.0%], respectively (Figure 3C,E). DMSO-treated colonoid nonresponders exhibited ΔA_{max} values of 2.2% [0.5%, 6.0%] (Figure 3D,E). The maximum nonresponder ΔA_{max} was 20.5%, with 48% of forskolin-treated colonoids exceeding this swelling amount (8 nonresponders and 24 responders out of 66 total forskolin-treated colonoids) (Figure 3E). These data demonstrate the heterogeneity of colonoid swelling, even in response to the same stimulus, forskolin, a direct activator of adenylyl cyclase.

induced swelling using colonoids derived from four wild-type mice (3 male, 1 female) was investigated (Figure S2). Arrayed colonoids grown from these mice were treated with forskolin, while a control well received 0.1% DMSO-containing medium only. The median ΔA_{max} of forskolin-treated colonoids from the four mice were 28.8% [20.5%, 33.1%], 15.1% [8.5%, 24.2%], 7.5% [2.7%, 14.5%], and 20.2% [9.4%, 28.8%], while the matching ΔA_{max} values for the DMSO control from these mice were 7.4% [4.3%, 10.3%], 5.6% [3.3%, 9.9%], 2.4% [0.9%, 4.9%], and 4.1% [0.1%, 6.9%], respectively. The mean ΔA_{max} of all three samples was significantly different from their respective DMSO controls (two-way ANOVA, $p < 10^{-7}$ for all comparisons) as well as between all four mice except between mice 1 and 4 ($p < 0.05$ for all comparisons) (Figure S2). While a functional variation between animal tissue can be expected, colonoid swelling did increase across all forskolin-treated samples relative to the paired DMSO control.

The dose dependence of forskolin-induced swelling in arrayed colonoids was then investigated and compared to that of embedded cultures using colonoids from the same mouse. Both arrayed and embedded colonoids demonstrated dose-dependent swelling for forskolin concentrations of 50 nM to 5 μM (Figure S3A). The dose responses were fit to sigmoidal logistic functions by nonlinear regression with least-squares estimation (Figure S3B). For arrayed colonoids, the EC_{50} and maximal relative area increase of forskolin-induced swelling were 175.7 nM (95% confidence interval (CI) = [52.4 nM, 299.0 nM]) and 344% (95% CI = [279%, 410%]), respectively. These metrics were not significantly different from the EC_{50} and maximum response of embedded colonoids from the same mouse, which were 232.4 nM (95% CI = [106.9 nM, 357.9 nM]) and 284% (95% CI = [248%, 321%]), respectively. Thus, overall forskolin-induced swelling in arrayed colonoids was similar to that of hydrogel-embedded cultures.

The dose-dependent response to forskolin permits an estimate of the number of colonoids needed to obtain a statistically significant swelling response as the forskolin concentration is altered. The lowest forskolin concentration that induced a statistically different response relative to the control was 250 nM ($p < 0.001$, two-way ANOVA), which induced 2.1- and 2.6-fold increases in median ΔA_{max} over the DMSO control for embedded and arrayed colonoids, respectively. Based on these data, the estimated total sample size required to detect statistically significant differences between the ΔA_{max} of forskolin and DMSO-treated colonoids is 2868 for the expected 1.2× difference, 322 for a 1.5× difference, 80 for a 2.8× difference, and 42 for a 2.9× difference. Thus, even for a moderate level of swelling (1.5-fold size increase), hundreds of colonoids must be screened for statistical confidence. The use of arrayed organoid strategy enables the assay of sufficient colonoids for these biologically relevant swelling conditions.

Investigation of Fluid Secretion by Cholera Toxin

Cholera is a well-known toxin that causes persistent diarrhea through cAMP production as well as activation of enteric nervous and immune systems. The toxin consists of two units, A and B. The combined toxin A + B (CT) is required to activate adenylyl cyclase and produce cAMP.(1) The B subunit of cholera toxin (C-B) binds to intestinal epithelial cells but does not stimulate cAMP production.(33) The impact of cholera toxin on colonoid arrays was investigated by adding CT, C-B, or medium to the cultures and applying the automated platform to track the colonoids over time. CT at both 0.5 and 5 μg/mL induced a significantly greater increase in ΔA_{max} than the medium-only control or 0.5 or 5 μg/mL C-B ($p < 0.01$ for all comparisons; Figure 4A). There was no statistical difference between wells treated with medium alone and wells treated with 0.5 or 5 μg/mL C-B (Figure 4A). These data demonstrate the utility of our platform in the measurement of cellular responses to enterotoxins.

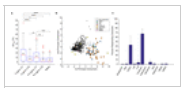

Figure 4. Colonoid swelling initiated by CT and compounds associated with the enteric nervous and immune systems. (A) Box-and-whisker plots of the maximal area attained by colonoids as a percentage of their area at time zero. The colonoids were incubated with CT or its B subunit at the indicated concentrations for 1.5 h. Colonoid responses to CT, C-B, and assay medium was statistically compared. (B) Two-dimensional reduction of a 10-dimensional colonoid data set using principal component analysis. The data set consisted of 768 colonoids across 16 wells of a 96-well plate treated with eight compounds and four controls. For clarity, the nonresponding colonoids in negative control medium are omitted. All nonresponding colonoids are shown in black, whereas colonoids with forskolin-like swelling responses are shown color-coded by treatment compound. (C) Proportion of colonoids that exhibit swelling within a 32 min window in response to compound treatment. Error bars represent ±1 standard deviation for three replicate experiments. A support vector machine (SVM) classifier was trained for each replicate experiment by using that replicate's forskolin-treated and control colonoids as the classification's positive and negative training groups, respectively.

Cell–enterotoxin interactions can activate enteric nervous and immune systems to produce compounds that induce ion transport or inhibit ion absorption, with subsequent water movement producing diarrhea and significant water loss through the colon.(1) To investigate the potency of such compounds on fluid transport on intestinal cells, eight compounds [bradykinin, prostaglandin E2, vasoactive intestinal peptide (VIP), adenosine, serotonin, acetylcholine, and histamine] generated by enteric nerves or inflammatory cells during infectious diarrhea were selected for screening on the primary arrayed colonoids (Table S1).(1) Colonoids at day 2 of culture were incubated with each compound for 32 min while undergoing time-lapse imaging. Forskolin was used as a positive control, while culture medium and C-B were included as negative controls. Automated image analysis enabled each colonoid's size, swelling magnitude, and swelling kinetics to be quantified by a panel of 10 metrics (Supporting Information). We then proceeded to analyze this rich data set for unique subpopulations. Support vector machine (SVM) classification was used to distinguish between responsive and nonresponsive colonoids. For each well-plate replicate, the forskolin-treated positive controls and standard medium negative controls were used to train a linear SVM binary classifier, which had an estimated accuracy of 91.3%–94.5% when distinguishing between swelling responders and static nonresponders. The effects of the screened compounds on individual colonoid area and resulting classification for a single well plate are shown in Figure S4. For the PGE2-treated sample, a large number of colonoids were identified as responders (49.6% ± 17.9%, total 70 out of 139) (Figure 4 B,C, Video S4). This PGE2-responsive subpopulation possessed a greatly increased median ΔA_{max} (16.2%) compared to that of PGE2 nonresponders (median ΔA_{max} 4.6%). PGE2 is known to be produced during infection with *Vibrio cholerae*(34), leading to an increase in cAMP.(35) These results show that colonoids in the cultures were not functionally equal. Previously, Magness and co-workers(36) have shown the transcriptional heterogeneity of small intestinal organoids within the same culture. Small numbers of colonoids treated with compounds other than forskolin or PGE2 were classified as responders (1.9%, or 37 out of 1955 colonoids) (Figure 4B,C). These responding colonoids could represent unique subpopulations within colonoids, but larger numbers of colonoids would need to be tracked to ascertain whether such subpopulations exist. Overall, these data support the utility of the arrayed colonoids when combined with automated imaging and computation as a screening platform to identify the intestinal response to exogenous compounds such as drugs and toxins.

Conclusions

This paper demonstrates the development of an arrayed colonoid culture system on the surface of a hydrogel support. The colonoids resided on a locally flat surface such that efficient automated imaging was possible by use of a computer-controlled microscope. Moreover, the cell types and polarity of the arrayed organoids were indistinguishable from hydrogel-embedded organoids. Using simple and accessible automated image analysis methods, we demonstrated the measurement of individual colonoid positions and sizes over time frames as long as 72 h. By this approach, net fluid movement across the epithelial cell monolayer of the organoids was tracked and quantified by using the colonoid cross-sectional area as a proxy. This image-based tracking of organoid swelling was used to screen a small set of physiological molecules associated with the enteric nervous and immune system for their impact on water movement across the colonoid epithelium. Heterogeneity in organoid response to chemicals, such as forskolin and PGE2, and toxins, such as cholera, was readily observed. For example, PGE2-treated colonoids displayed a responsive subpopulation that possessed 3.5× higher response compared to that of PGE2 nonresponders. To detect smaller swelling responses, from 1- to 2-fold that of the control, hundreds to thousands of colonoids are required to identify statistically significant responses. This arrayed colonoid system readily permits large numbers of organoids to be assayed, thus allowing small subpopulations to be identified. In this instance, 2248 colonoids were assayed in less than 4 h for the compound screen. We anticipate the utility of this arrayed colonoid culture for applications involving screens of drugs, bacterial products, and dietary metabolites on primary intestinal tissue. Further, we anticipate that this platform can be readily extended to culture human intestinal organoids for personalized medicine applications.

Supporting Information

The Supporting Information is available free of charge on the ACS Publications website at DOI: 10.1021/acs.analchem.7b04032.

- Additional text describing clustering analyses for determination of colonoid heterogeneity; two figures showing

dependence of forskolin-induced swelling, and PCA of compound-induced colonoid swelling; one table listing compounds screened for impact on colonoid swelling (PDF)

- Video S1 (AVI)
- Video S2 (AVI)
- Video S3 (AVI)
- Video S4 (AVI)

PDF

- ac7b04032_si_001.pdf (1.4 MB)

Microsoft Video (AVI)

- ac7b04032_si_002.avi (1.87 MB)
- ac7b04032_si_003.avi (454.2 kB)
- ac7b04032_si_004.avi (474.29 kB)
- ac7b04032_si_005.avi (244.73 kB)

Development of Arrayed Colonic Organoids for Screening of Secretagogues Associated with Enterotoxins

Showing 1/5: ac7b04032_si_001.pdf

Supporting Information

Development of arrayed colonic organoids for screening of secretagogues associated with enterotoxins

Dulan B. Gunasekara[1§], Matthew DiSalvo[2§], Yuli Wang[1], Daniel L. Nguyen[1], Mark I. Reed[1], Jennifer Speer[1], Christopher E. Sims[1], Scott T. Magness[2, 3], Nancy L. Allbritton[1, 2, *]

[1]Department of Chemistry, University of North Carolina at Chapel Hill, NC 27599, USA

[2]Joint Department of Biomedical Engineering, University of North Carolina at Chapel Hill, NC 27599, USA and North Carolina State University, Raleigh, NC 27607, USA.

[3]Department of Medicine, Division of Gastroenterology and Hepatology, University of North Carolina, Chapel Hill, NC 27599, USA

figshare 1 / 5 Share Download

‖Author Contributions
D.B.G. and M.D. contributed equally to this work.

The authors declare the following competing financial interest(s): N.L.A., Y.W., C.E.S., S.T.M., have a financial interest in Altis Biosystems LLC.

Acknowledgment

Research reported in this publication was supported by the National Institutes of Health under Award R01DK109559 to N.L.A. and S.T.M. and by UNC translational team science award under CTSA Grant UL1TR001111 (S.T.M.). We thank Ian Williamson for coordinating the procurement of mouse colons.

References

1. Field, M. *J. Clin. Invest.* **2003**, 111, 931– 943 DOI: 10.1172/JCI200318326 [Crossref], [PubMed], [CAS]
2. O'Neal, C. J.; Jobling, M. G.; Holmes, R. K.; Hol, W. G. *Science* **2005**, 309, 1093– 1096 DOI: 10.1126/science.1113398 [Crossref], [PubMed], [CAS]
3. Hodges, K.; Gill, R. *Gut Microbes* **2010**, 1, 4– 21 DOI: 10.4161/gmic.1.1.11036 [Crossref], [PubMed], [CAS]
4. Greger, R. *Annu. Rev. Physiol.* **2000**, 62, 467– 491 DOI: 10.1146/annurev.physiol.62.1.467 [Crossref], [PubMed], [CAS]
5. Thiagarajah, J. R.; Verkman, A. *Curr. Opin. Pharmacol.* **2013**, 13, 888– 894 DOI: 10.1016/j.coph.2013.08.005 [Crossref], [PubMed], [CAS]
6. Muanprasat, C.; Chatsudthipong, V. *Future Med. Chem.* **2013**, 5, 781– 798 DOI: 10.4155/fmc.13.42 [Crossref], [PubMed], [CAS]
7. Grabinger, T.; Luks, L.; Kostadinova, F.; Zimberlin, C.; Medema, J. P.; Leist, M.; Brunner, T. *Cell Death Dis.* **2014**, 5e1228 DOI: 10.1038/cddis.2014.183 [Crossref], [PubMed]
8. Shamir, E. R.; Ewald, A. J. *Nat. Rev. Mol. Cell Biol.* **2014**, 15, 647– 664 DOI: 10.1038/nrm3873 [Crossref], [PubMed], [CAS]
9. Ranga, A.; Gjorevski, N.; Lutolf, M. P. *Adv. Drug Delivery Rev.* **2014**, 69–70, 19– 28 DOI: 10.1016/j.addr.2014.02.006 [Crossref], [PubMed], [CAS]
10. Sato, T.; Vries, R. G.; Snippert, H. J.; van de Wetering, M.; Barker, N.; Stange, D. E.; van Es, J. H.; Abo, A.; Kujala, P.; Peters, P. J.; Clevers, H. *Nature* **2009**, 459, 262– 265 DOI: 10.1038/nature07935 [Crossref], [PubMed], [CAS]
11. Dekkers, J. F.; Wiegerinck, C. L.; de Jonge, H. R.; Bronsveld, I.; Janssens, H. M.; de Winter-de Groot, K. M.; Brandsma, A. M.; de Jong, N. W. M.; Bijvelds, M. J. C.; Scholte, B. J.; Nieuwenhuis, E. E. S.; van den Brink, S.; Clevers, H.; van der Ent, C. K.; Middendorp, S.; Beekman, J. M. *Nat. Med.* **2013**, 19, 939– 945 DOI: 10.1038/nm.3201 [Crossref], [PubMed], [CAS]
12. Yamada, K. M.; Cukierman, E. *Cell* **2007**, 130, 601– 610 DOI: 10.1016/j.cell.2007.08.006 [Crossref], [PubMed], [CAS]
13. Debnath, J.; Brugge, J. S. *Nat. Rev. Cancer* **2005**, 5, 675– 688 DOI: 10.1038/nrc1695 [Crossref], [PubMed], [CAS]
14. Zietek, T.; Rath, E.; Haller, D.; Daniel, H. *Sci. Rep.* **2015**, 516831 DOI: 10.1038/srep16831 [Crossref], [PubMed], [CAS]
15. Mizutani, T.; Nakamura, T.; Morikawa, R.; Fukuda, M.; Mochizuki, W.; Yamauchi, Y.; Nozaki, K.; Yui, S.; Nemoto, Y.; Nagaishi, T., et al. *Biochem. Biophys. Res. Commun.* **2012**, 419, 238– 243 DOI: 10.1016/j.bbrc.2012.01.155 [Crossref], [PubMed], [CAS]
16. Schwank, G.; Koo, B.-K.; Sasselli, V.; Dekkers, J. F.; Heo, I.; Demircan, T.; Sasaki, N.; Boymans, S.; Cuppen, E.; van der Ent, C. K.; Nieuwenhuis, E. E. S.; Beekman, J. M.; Clevers, H. *Cell Stem Cell* **2013**, 13, 653– 658 DOI: 10.1016/j.stem.2013.11.002 [Crossref], [PubMed], [CAS]
17. Jin, B.-J.; Battula, S.; Zachos, N.; Kovbasnjuk, O.; Fawlke-Abel, J.; In, J.; Donowitz, M.; Verkman, A. S. *Biomicrofluidics* **2014**, 8024106 DOI: 10.1063/1.4870400 [Crossref], [PubMed], [CAS]
18. Moon, C.; Zhang, W.; Ren, A.; Arora, K.; Sinha, C.; Yarlagadda, S.; Woodrooffe, K.; Schuetz, J. D.; Valasani, K. R.; de Jonge, H. R.; Shanmukhappa, S. K.; Shata, M. T. M.; Buddington, R. K.; Parthasarathi, K.; Naren, A. P. *J. Biol. Chem.* **2015**, 290, 11246– 11257 DOI: 10.1074/jbc.M114.605410 [Crossref], [PubMed], [CAS]
19. Fujii, S.; Suzuki, K.; Kawamoto, A.; Ishibashi, F.; Nakata, T.; Murano, T.; Ito, G.; Shimizu, H.; Mizutani, T.; Oshima, S.; Tsuchiya, K.; Nakamura, T.; Araki, A.; Ohtsuka, K.; Okamoto, R.; Watanabe, M. *Sci. Rep.* **2016**, 636795 DOI: 10.1038/srep36795 [Crossref], [PubMed], [CAS]
20. Foulke-Abel, J.; In, J.; Kovbasnjuk, O.; Zachos, N. C.; Ettayebi, K.; Blutt, S. E.; Hyser, J. M.; Zeng, X.-L.; Crawford, S. E.; Broughman, J. R.; Estes, M. K.; Donowitz, M. *Exp. Biol. Med.* **2014**, 239, 1124– 1134 DOI: 10.1177/1535370214529398 [Crossref], [CAS]
21. Spence, J. R. *Cell. Mol. Gastroenterol. Hepatol.* **2017**, 4, 203– 204 DOI: 10.1016/j.jcmgh.2017.04.006 [Crossref], [PubMed], [CAS]
22. Wang, Y.; DiSalvo, M.; Gunasekara, D. B.; Dutton, J.; Proctor, A.; Lebhar, M. S.; Williamson, I. A.; Speer, J.; Howard, R. L.; Smiddy, N. M., et al. others *Cell. Mol. Gastroenterol. Hepatol.* **2017**, 4, 165– 182 DOI: 10.1016/j.jcmgh.2017.02.011 [Crossref], [PubMed], [CAS]
23. Gracz, A. D.; Ramalingam, S.; Magness, S. T. *AJP Gastrointest. Liver Physiol.* **2010**, 298, G590– G600 DOI: 10.1152/ajpgi.00470.2009 [Crossref], [PubMed]
24. Ahmad, A. A.; Wang, Y.; Gracz, A. D.; Sims, C. E.; Magness, S. T.; Allbritton, N. L. *J. Biol. Eng.* **2014**, 89 DOI: 10.1186/1754-1611-8-9 [Crossref], [PubMed], [CAS]
25. Miyoshi, H.; Stappenbeck, T. S. *Nat. Protoc.* **2013**, 8, 2471– 2482 DOI: 10.1038/nprot.2013.153 [Crossref]

Ramalingam, S.; Daughtridge, G. W.; Johnston, M. J.; Gracz, A. D.; Magness, S. T. *Am. J. Physiol. - Gastrointest. Liver Physiol.* **2012**, 302, G10– G20 DOI: 10.1152/ajpgi.00277.2011 [Crossref], [PubMed]

27. Otsu, N. *IEEE Trans. Syst. Man Cybern.* **1979**, 9, 62– 66 DOI: 10.1109/TSMC.1979.4310076 [Crossref]
28. Roerdink, J. B.; Meijster, A. *Fundam. Informaticae* **2000**, 41, 187– 228
29. Schölkopf, B.; Smola, A. J. *Learning with Kernels: Support Vector Machines, Regularization, Optimization, and Beyond*; MIT Press: **2002**.
30. Rao, M. C.; Sarathy, J.; Sellin, J. H. In *Sleisenger and Fordtran's Gastrointestinal and Liver Disease*; Elsevier: **2016**; pp 1713– 1735.
31. Debnath, J.; Muthuswamy, S. K.; Brugge, J. S. *Methods* **2003**, 30, 256– 268 DOI: 10.1016/S1046-2023(03)00032-X [Crossref], [PubMed], [CAS]
32. Ubelmann, F.; Chamaillard, M.; El-Marjou, F.; Simon, A.; Netter, J.; Vignjevic, D.; Nichols, B. L.; Quezada-Calvillo, R.; Grandjean, T.; Louvard, D.; Revenu, C.; Robine, S. *Proc. Natl. Acad. Sci. U. S. A.* **2013**, 110, E1380– E1389 DOI: 10.1073/pnas.1218446110 [Crossref], [PubMed], [CAS]
33. Sánchez, J.; Holmgren, J. *Indian J. Med. Res.* **2011**, 133, 153– 163[PubMed], [CAS]
34. Hecht, G. *Am. J. Physiol.-Cell Physiol.* **1999**, 277, C351– C358 DOI: 10.1152/ajpcell.1999.277.3.C351 [Crossref], [PubMed], [CAS]
35. Dey, I.; Lejeune, M.; Chadee, K. *Br. J. Pharmacol.* **2006**, 149, 611– 623 DOI: 10.1038/sj.bjp.0706923 [Crossref], [PubMed], [CAS]
36. Gracz, A. D.; Williamson, I. A.; Roche, K. C.; Johnston, M. J.; Wang, F.; Wang, Y.; Attayek, P. J.; Balowski, J.; Liu, X. F.; Laurenza, R. J.; Gaynor, L. T.; Sims, C. E.; Galanko, J. A.; Li, L.; Allbritton, N. L.; Magness, S. T. *Nat. Cell Biol.* **2015**, 17, 340– 349 DOI: 10.1038/ncb3104 [Crossref], [PubMed], [CAS]

Related Content

Nonsteroidal Anti-Inflammatory Drug-Induced Leaky Gut Modeled Using Polarized Monolayers of Primary Human Intestinal Epithelial Cells
ACS Infectious Diseases
Bhatt, Gunasekara, Speer, Reed, Peña, Midkiff, Magness, Bultman, Allbritton, and Redinbo
2018 *4* (1), pp 46–52
Abstract | Full Text HTML | PDF w/ Links | Hi-Res PDF

Design and Application of Sensors for Chemical Cytometry
ACS Chemical Biology
Vickerman, Anttila, Petersen, Allbritton, and Lawrence
2018 *13* (7), pp 1741–1751
Abstract | Full Text HTML | PDF w/ Links | Hi-Res PDF

***In Vitro* Generation of Mouse Colon Crypts**
ACS Biomaterials Science & Engineering
Wang, Gunasekara, Attayek, Reed, DiSalvo, Nguyen, Dutton, Lebhar, Bultman, Sims, Magness, and Allbritton
2017 *3* (10), pp 2502–2513

Partners